Suitability of Polyvinyl Alcohol Cryogel as a Tissue-Mimicking, Artificial Lumbar Intervertebral Disc

Wang, William Hao; Campbell, Gord

Publisher's version / Version de l'éditeur:

Spine, 34, 25, pp. 45-53, 2009-12-01

Title Page

Title:

Suitability of Poly Vinyl Alcohol Cryogel as a Tissue-Mimicking, Artificial Lumbar Intervertebral Disc.

Authors:

William Hao Wang, MD Candidate

Affiliations:

Schulich School of Medicine and Dentistry, The University of Western Ontario, London, Ontario, Canada

Gord Campbell, PhD, PEng

Affiliations:

National Research Council – London, Ontario, Canada

Department of Medical Biophysics, Schulich School of Medicine and Dentistry, The University of Western Ontario, London, Ontario, Canada

Department of Mechanical and Materials Engineering, Faculty of Engineering, The University of Western Ontario, London, Ontario, Canada

Correspondence:

Dr. Gord Campbell
NRC-London
800 Collip Circle
London, Ontario
Canada N6G 4X8
Tel: (519) 430-7079
Fax: (519) 430-7032
Gordon.Campbell@nrc-cnrc.gc.ca

Funding:

National Research Council Canada (NRC)
Summer Research Training Program (SRTP) – Schulich School of Medicine and Dentistry (pooled funding sources)

Acknowledgement:

We would like to thank the following surgeons for their insight and assistance:

Dr. Kevin Gurr, Associate Prof., MD.
Dr. Christopher Bailey, Assistant Prof., MD.

Affiliations:

Department of Surgery, Schulich School of Medicine and Dentistry, The University of Western Ontario, London, Ontario, Canada;
Department of Orthopedic Surgery, London Health Sciences Center, London, Ontario, Canada

Structured Abstract

Study Design. An original investigation that characterizes poly (vinyl alcohol) cryogel (PVA-C) in the context of the human lumbar intervertebral disc.

Objectives. To evaluate the mechanical properties of PVA-C under physiological conditions; to assess PVA-C's suitability as a tissue-mimicking artificial lumbar intervertebral disc material; and to identify suitable formulations that mimic the nucleus pulposus and annulus fibrosus.

Summary of Background Data. Current lumbar intervertebral disc prostheses provide suboptimal symptom relief and do not restore natural load-cushioning. PVA-C is a promising material due to its high water content, excellent biocompatibility, and versatile mechanical properties.

Methods. PVA-C samples were prepared with different PVA concentrations and number of freeze-thaw cycles (FTC). Unconfined compression was conducted to characterize various PVA-C formulations. Compressive stress relaxation and creep were performed to assess the stability of PVA-C under loading. The results were compared with the mechanical properties of human lumbar intervertebral discs obtained from the literature.

Results. PVA-C compressive elastic modulus increased with increasing PVA concentration and number of FTC's. The 3%-3FTC is the optimal formulation for

mimicking the nucleus pulposus. In general, compressive stress relaxation and creep decreased with increasing PVA concentration and number of FTC's. Compressive stress relaxation and creep were lower for PVA-C than human lumbar intervertebral discs, suggesting that PVA-C will likely exhibit stable and predictable mechanical response *in-vivo*. Current formulations did not have adequate compressive elastic modulus to mimic the annulus fibrosus.

Conclusion. The 3%-3FTC PVA-C formulation is likely the optimal choice for a tissue mimicking artificial nucleus pulposus. Good compressive stress relaxation and creep behavior, combined with excellent biocompatibility, makes PVA-C a suitable choice for a tissue-mimicking artificial IVD. Future investigations will focus on increasing the stiffness of PVA-C by approximately an order of magnitude in order to mimic the material properties of the annulus fibrosus.

Key Words

intervertebral disc, artificial, lumbar, poly (vinyl alcohol), PVA, compression, creep, stress relaxation

Key Points

- Current lumbar intervertebral disc prosthesis provide suboptimal symptom relief and do not restore the natural load cushioning ability of the intervertebral joint
- PVA-C is a promising material for a new tissue-mimicking artificial intervertebral disc

- Future work will focus on finding a suitable formulation to replace the annulus fibrosus.

Mini Abstract

PVA-C is a promising material for a new tissue-mimicking artificial lumbar intervertebral disc. The material properties of PVA-C were characterized for this purpose. PVA-C has good compressive stress relaxation and creep behaviors; the 3% PVA formulation with 3 freeze-thaw cycles is optimal for replacing the nucleus pulposus.

Text

Introduction:

Mechanical low back pain is one of the most ubiquitous health care problems in modern society; it remains the second most common reason for lost work productivity and physician office visits.[2,5-8] Injury or degeneration of the intervertebral disc (IVD) has been implicated as one of the major causes of low back pain, and some patients will eventually require surgical intervention.[5-8] Most commonly, spinal fusion (arthrodesis) is performed. However, a systematic review has found that disability outcomes between fusion and nonsurgical intervention did not meet FDA's criteria for clinically meaningful difference.[9] Artificial lumbar disc replacement is a newer alternative to fusion.[10] To date, only the Charite artificial disc and ProDisc-L are approved by the FDA and undergone randomized clinical trial. The outcome showed that both systems had slightly better short-term disability outcomes when compared to lumbar fusion, however these benefits diminished at 24 months.[11,12] It is safe to say that regardless of the relative benefit of fusion, disc replacement, or nonsurgical intervention, few patients achieve complete symptom resolution after any of these treatments. This leaves much room for improvement in artificial intervertebral disc designs.

The human IVD functions primarily to bear and distribute loads as well as dissipate energy.[1] It performs these functions exceedingly well due to its unique composition of a soft proteoglycan-rich inner core called nucleus pulposus and a tough collagen-rich outer shell called annulus fibrosus.[1-4] An ideal artificial intervertebral disc should restore normal joint biomechanics, particularly the load-cushioning ability.[2,7,13] The current

prosthetic devices offer suboptimal solutions due to their stiff titanium and ultrahigh molecular weight polyethylene (UHMWPE) construction and unnatural range of motion. Furthermore, the titanium-UHMWPE articulation exhibits the same problems of wear and debris accumulation as hip and knee joint implants, which causes undesirable inflammatory reactions.[14]

The appropriateness of poly (vinyl alcohol) cryogels (PVA-C) for biomedical applications has been recognized due to its high water content, excellent biocompatibility and versatile mechanical properties.[21] PVA has been investigated as a material for artificial articular cartilage,[15-20] contact lens,[21-24] and nucleus pulposus replacement.[2,25-27]

While previous studies have investigated nucleus pulposus replacements with PVA hydrogels,[2,25-27] none have considered using multiple PVA-C formulations to replace the whole disc in order to mimic the mechanical behavior of the natural tissues. The new design would involve assembling components with different formulations of PVA-C's to form a structure almost identical to the natural IVD. The aim of this paper is to characterize and evaluate the mechanical properties of PVA-C formulations at various concentrations and freeze-thaw cycles under physiological conditions with respect to its suitability as an artificial lumbar intervertebral disc material.

Methods:

Sample Preparation

PVA (99% hydrolyzed, 124,000–164,000 MW, Aldridge Chemical Co., Inc.) was dissolved in deionized water at 70-90°C for 2-3 hours to obtain 3%, 5%, 15%, 25%, 35%, 40% w/w PVA solutions. The solutions were poured into molds to create samples with a flat disk shape (38mm diameter, 12mm height). The samples were temperature cycled from +20°C, to -20°C, to +20°C at 0.1°C/min, representing one complete freeze-thaw cycle (FTC). Each concentration of PVA solution underwent 1, 3 or 6 FTC's.

Mechanical tests were carried out using an MTS 858-Bionix servohydraulic material testing system with FlexTest SE controller. All tests were performed in water heated to 37°C.

Unconfined Compression

Literature search revealed that the full range of physiologic loads experienced by the whole human IVD is quite variable. Therefore the PVA-C samples were loaded in displacement-controlled mode to yield more meaningful data.

The magnitude of displacement was calculated to encompass the deformation experienced by the IVD both during normal daily activities and maximum tolerable physiologic loading. Data extrapolated from existing literature indicate that during normal walking, the range of deformation of the human IVD (expressed as % strain) is approximately 5-10%.[4,28,29] The maximum deformation under "unfavourable" loading of the lumbar IVD was calculated to be approximately 4400N.[1] This value corresponds to a strain of 15-25%.[4,29] This maximum load was validated by the fact that the vertebral

endplates typically fails at approximately 4000-6000N.[29] A 3mm displacement, corresponding to approximately 25% strain in PVA-C, was chosen.

A slow crosshead speed of 2mm/min was chosen to facilitate easier comparison between the PVA-C and human IVD data. The PVA-C samples were loaded to 3mm and then immediately unloaded. Tangent compressive elastic moduli were calculated at 5% and 20% strain, corresponding to the aforementioned deformation levels. Preconditioning was performed on all samples.

Compressive Stress Relaxation

Compressive stress relaxation tests used 3mm displacement magnitude with 4mm/s crosshead speed. The crosshead speed was derived based on human IVD load profile during "very fast" walking (2.16m/s) to simulate fast deformations that may arise on a daily basis.[1,30] The displacement was held for 30seconds before unloading. Preliminary studies (data not shown) confirmed that stress relaxation reached steady state values after 30 seconds and that longer time periods (upto 20min) did not contribute to significant changes in relaxation rate. The instantaneous stress relaxation rate, final stress relaxation rate, and percent change in stress were calculated. The load-time data were then curve fitted by Eq. (1) as described by Wan et al:[31]

$$\frac{\sigma_1}{\sigma_0} = \sigma_R + \alpha e^{-k_1 t} + \beta e^{-k_2 t} \qquad (1)$$

σ_1 is stress at time t, σ_0 is the initial stress at t=0 seconds, σ_R is the final relative remaining stress at t=30 seconds, α and β are proportional constants for the crystalline

and amorphous regions, k_1 and k_2 are relaxation-rate fitting parameters for the initial and final regions respectively.

Compressive Creep

Compressive creep tests were performed by applying an initial load that corresponds to a load that would cause 3mm of displacement or 223N, which ever is lower (due to sensor limitations). A loading time of approximately 0.8sec was used, corresponding to the 4mm/s deformation rate. Instantaneous and steady state creep rates, as well as percent change values were calculated. The strain-time data was curve fitted using the exact parametric solution equations derived from a "three-parameter-solid" model shown in Eq. (2).[32-34]

$$\frac{\varepsilon(t)}{\sigma_0} = \frac{1}{E_1}\left(1 - e^{-\frac{E_1}{\eta}t}\right) + \frac{1}{E_2} \qquad (2)$$

E_1 and E_2 are the viscous (equilibrium) and elastic (instantaneous) modulus, respectively, and η is the viscosity. This model has been validated on human lumbar IVD's.[32,34]

Both curve fitting procedures used the nonlinear least squares fitting method to minimize the summed squares of residuals. This was implemented using the Trust-region algorithm in MATLAB with 95% confidence interval.

Results:

Unconfined Compression

Figure 1 shows a typical set of stress-strain hysteresis curves at 3mm displacement loading for 15%PVA-C 1, 3 and 6FTC. Note the classic nonlinear elastic (more specifically, viscoelastic) response that is characteristic of PVA-C as well as most human soft tissues. The initial phase of unloading followed a different path than the loading phase (typical hysteresis). The loading and unloading paths eventually converged to the same starting point, thereby avoiding any permanent plastic deformation. This temporary hysteresis is probably due to a lag in entropic elastic recovery.[35,36] Fluid diffusion in liquid phase of the gel may also have contributed (i.e. poroelasticity).[37]

The initial tangent compressive elastic modulus at 5% strain and large tangent compressive elastic modulus at 20% strain both increased with increasing PVA concentration and increasing number of FTC's (Figures 2, 3 and Table 1). This is consistent with existing literature regarding PVA-C.[21,38-40] Increasing PVA concentration is associated with higher degree of crystallinity,[40] while increasing number of FTC's is associated with coarsening of regions of heterogeneity and increasing consolidation of polymer chain entanglement.[40] Overall, the PVA-C formulations exhibited a wide range of elastic modulus values. The initial elastic modulus values ranged from 0.70kPa (3%-1FTC) to 1.30MPa (40%-6FTC). The large elastic modulus values ranged from 1kPa (3%-1FTC) to 2.12MPa (40%-6FTC).

Compressive Stress Relaxation

Figure 4 shows the stress relaxation data for the 35%-3FTC sample accompanied by its Eq. (1) curve fitting. Figure 5 shows the instantaneous stress relaxation rates, which ranged from 30Pa/s (3%-1FTC) to 109.5kPa/s (40%-6FTC). The instantaneous stress relaxation rates increased dramatically with increasing PVA concentration and number of FTC's, spanning approximately 4 orders of magnitude. The final stress relaxation rates ranged from 0.2Pa/s (3%-1FTC) to 100Pa/s (40%-6FTC). The final stress relaxation rates for all formulations spanned a narrower range than the instantaneous rates. Although, the final stress relaxation rates increased with increasing PVA concentration and number of FTC's, they plateaued at high PVA concentrations, indicating that the rates were likely converging to a common value. The percent changes in stress were less than 20%. Table 2 provides a summary of stress relaxation results.

The fitting parameters k_1 and k_2 represent the slopes of the relaxation curve during the initial and final times respectively. Upon inspection of data, neither k_1 nor k_2 values appeared to exhibit any correlation with PVA-C concentration or number of FTC's. Most k_1 values were comparable to each other, as were k_2 values. This was likely a result of the normalization process. In addition, the proportionality constants α and β probably also played a role in shaping the fitted curves. This suggests that stress relaxation of hard and soft PVA formulations are scaled versions of one another.

Compressive Creep

Figure 6 shows the creep data for the 15%-3FTC sample accompanied by its Eq. (2) curve fitting. The instantaneous creep rate ranged from $0.013sec^{-1}$ (3%-6FTC, sec=seconds) to $0.0044sec^{-1}$ (40%-6FTC). The final creep rate ranged from $8x10^{-5}sec^{-1}$ (3%-6FTC) to $2x10^{-5}sec^{-1}$ (40%-6FTC). The final creep rates were less than $10^{-4}sec^{-1}$ for all formulations, indicating that creep rates likely converged toward a common value. The percent changes in strain were comparable amongst different formulations within experimental error. Except for the 3%-6FTC and 5%-3FTC formulations, the percent change values ranged from 1.4% to 3.6%. Table 3 provides a summary of creep results. Creep measurements from 3%-1FTC, 3%-3FTC, and 5%-1FTC samples were not reported due to the exceedingly low forces involved, which surpassed the control limitations of the material testing system.

Figure 7 and 8 and Table 3 show values of Eq. (2) fitting parameters E_1, E_2 and η. E_2 is the instantaneous elastic modulus which dictates the instantaneous response (t=0 seconds) of the samples to the applied loads. E_1 and η characterizes the Kelvin body,[32-34] and their effects are seen at equilibrium (t>>0 seconds) adding to the effects of E_2. E_2 values increased with increasing PVA concentration and number of FTC's. This is not surprising since the compressive elastic moduli in unconfined compression exhibited the same trend. Both E_1 and η also increased with increasing PVA concentration and number of FTC's. However, the trend is not as consistent for η. The E_1 and η trends indicate that samples with higher PVA concentrations and number of FTC's are more "viscous" and will undergo less creep when loaded.

Discussion:

The materials used in aritifical IVD designs to date can be divided into three general categories: metal, nonmetal, and composite.[2,14,41] The soft tissue components – annulus fibrosus and nucleus pulposus – are often replaced by an elastomer (e.g. polyurethane, polyolefin, silicone, polysiloxane, etc.) or a plastic (e.g. polyethylene). [2,14,41] Hydrogels are typically used for nucleus pulposus replacements, and so far only one design uses PVA (Aquarelle).[25,26] Although nuclear replacement alone may result in greater preservation of natural tissue, it has certain draw backs. Firstly, success of nucleus replacement may depend on severity of degeneration, with better results for earlier degeneration.[2,42,43] Discs with advanced degeneration may not be able to safely contain a nucleus implant, risking rupture of the remaining annulus fibers and/or endplates.[25,44] Secondly, the remaining disc tissues may continue the local inflammatory process, resulting in sub-optimal symptom control.[44] Thirdly, device migration, extrusion and catastrophic herniation are all possible due to lack of mechanical fixation to the annulus and endplates.[25,27] It is therefore desirable to use a tissue mimicking material like PVA-C to replicate the essential biomechanical properties of the natural IVD.

Comparison to Human IVD Data

Table 4 shows a summary of the human IVD properties[4,28,29,34,45-53] along with the closest matching PVA-C formulation(s). The human IVD exhibits the classic non-linear elastic load-displacement curve that's roughly "J-shaped" with an initial "toe" region followed by a steeper linear region.[28,29,45,46] The fact that PVA-C also exhibits this non-linear stress-strain response is a good indication that it could mimic the mechanical

response of human IVD's well. In general, tests performed on the human lumbar IVD's all showed much greater hysteresis than the PVA-C formulations,[4,29,46,48,49] since preconditioning tends to be much more critical for human IVD's than for PVA-C (data not shown). It is interesting to note that the human IVD tends to exhibit a significant amount of plastic deformation after the first loading cycle, but the plastic deformation diminished rapidly with subsequent loading cycles.[4,29,46] This usually amounts to less than 10% disc height loss. In comparison PVA-C does not exhibit this kind of cycle-dependent plastic deformation, suggesting good dimensional stability.

Upon inspection of data, the human IVD annulus fibrosus possesses greater compressive elastic modulus values than the current set of PVA-C formulations. For the nucleus pulposus, the 3%-3FTC and 5%-1FTC formulations provide the best match. Of the two, the 3%-3FTC formulation is likely better due to greater dimensional stability. The physical properties of PVA-C have been extensively investigated, and studies suggest that increased number of FTC's tends to decrease the amount of swelling and dissolution of PVA molecules upon submersion in water.[21,38] This is consistent with the authors' observations. The higher number of FTC's of the 3%-3FTC formulation has a greater influence on dimensional stability than the higher PVA concentration of 5%-1FTC formulation.

There is ongoing debate about whether the nucleus pulposus is really a liquid or a solid.[54,55] This question is difficult to answer due to age-dependent dehydration of the nucleus that occurs in human IVD. Furthermore the rate and degree of dehydration is

subject to individual variations.[2,56] Mechanical testing indicate that for a normal healthy human IVD, the nucleus pulposus would most likely behave like a viscous fluid under static loading, and like soft viscoelastic solid under dynamic loading.[54,55] The 3%-3FTC and 5%-1FTC formulations, behave more like viscoelastic solids under both loading conditions (data not shown). This was felt to be appropriate because solid-like behavior imparts stability and predictability under varying loads. It would be more difficult to achieve consistent mechanical responses if a fluid-like material is used due to liberal fluid diffusion in and out of the porous endplates.[2,27,57]

In stress relaxation, preliminary studies showed that given enough time (~20 minutes), the samples reach nearly zero relaxation rate. Stress relaxation tests performed on human cadaveric lumber IVD's showed that after a long period of constant deformation (30min – 1hr) the stress relaxation rates could eventually reached zero as well.[4] The percent change in stress for human lumbar IVD's depends on the amount of load applied (e.g. 100kg, 200kg, or 300kg) but tends to be much higher than values for PVA-C, often exceeding 50%.[4] The greater percent decrease is likely due to a combination of higher applied loads and inherent response of the disc itself. A tissue-mimicking artificial IVD should have equal or lower stress relaxation than the human IVD to provide a stable and predictable load-displacement relationship. The PVA-C stress relaxation results are encouraging since most PVA-C samples showed less than 10% decrease in stress. To date, scant literature exists that analyzes the stress relaxation of human IVD's using rigorous curve fitting methods. Thus, the parameters k_1 and k_2 calculated in this study could not be easily compared to human IVD data.

In creep, the human lumbar IVD's demonstrate a steady state non-zero creep rate even after a significant period of time (30min – 1hr).[4,34] Conversely, PVA-C data showed that creep rates tend to converge toward zero for all formulations. The percent change in displacement after extended loading for human IVD's were also higher than PVA-C results.[4,34] This is encouraging since a tissue-mimicking artificial IVD should have equal or lower creep rate than the human IVD in order to maintain dimensional stability under sustained loading. This is especially important in ensuring that the prosthesis will not deform to an unacceptable level during prolonged static loading and cause impingement on surrounding tissues – most notably the spinal cord and nerve roots. The E_1, E_2 and η values were generally lower than the values derived from human IVD data.[34] This was most likely due to the lower compressive elastic modulus of PVA-C compared to human IVD as mentioned previously. A few of the E_1 and E_2 values were comparable to human data, and the η values were generally low, however none of the formulations could match all three parameters simultaneously.

It is evident from Table 5 that future investigations should focus on finding a PVA-C formulation with adequate compressive elastic modulus to function as an artificial annulus fibrosus. Since further increase in PVA concentration is impractical, some preliminary work was performed to investigate composite PVA-C structures. Particle or fiber reinforced PVA-C structures are possible. As well, nucleating agents maybe used to further increase the degree of crystallinity and strength of PVA-C. Finally, the issue of endplate attachment was also considered, and bonded titanium mesh[58] or porous

titanium plate (unpublished data) are both promising options for PVA attachment. Both Charite and ProDisc use titanium endplates with mechanical features (spikes or keel) to facilitate bone in-growth and demonstrate satisfactory results.

Conclusion:

It was found that the 3%-3FTC PVA-C formulation is the optimal choice for a tissue mimicking artificial nucleus pulposus. It provides the best combination of mechanical properties and dimensional stability. Stress relaxation and creep comparisons with human IVD data showed that PVA-C underwent less stress relaxation and creep than human IVD, indicating that PVA-C should behave predictably over a wide range of loading conditions *in-vivo*. Combined with its excellent biocompatibility, this makes PVA-C a suitable choice for a tissue-mimicking artificial IVD.

Unfortunately, a completely suitable replacement for the annulus fibrosus could not be selected from the current formulations of homogeneous PVA-C. At the highest concentration of PVA-C tested (40%-6FTC), the material reached 10-15% of required elastic modulus. Future investigations will explore composite PVA-C formulations to boost stiffness by approximately an order of magnitude without compromising load-cushioning ability and toughness. Due to the choice in methodology to characterize PVA-C by elastic modulus rather than by maximum load, the PVA-C samples were not subjected to the same levels of maximum loads as human lumbar IVD's. Future tests on stiffer composite formulations will reveal the response of PVA-C under large physiologic loads, comparable to loads subjected to human IVD's.

References

1. Nordin M, Frankel V, Lindh M. Chapter 10 – Biomechanics of the Lumbar Spine. Basic Biomechanics of the Musculoskeletal System, Second Edition. 1989:183-207.

2. Bao QB, McCullen GM, Higham PA, et al. The artificial disc: theory, design and materials. Biomaterials 1996;17:1157-67.

3. Nachemson A. The load on lumbar disks in different positions of the body. Clin Orthop Relat Res 1966;45:107-22.

4. Markolf KL, Morris JM. The structural components of the intervertebral disc. A study of their contributions to the ability of the disc to withstand compressive forces. J Bone Joint Surg Am 1974;56:675-87.

5. Andersson GB. Epidemiologic aspects on low-back pain in industry. Spine 1981;6:53-60.

6. Kleinstueck FS, Diederich CJ, Nau WH, et al. Acute biomechanical and histological effects of intradiscal electrothermal therapy on human lumbar discs. Spine 2001;26:2198-207.

7. Hedman TP, Kostuik JP, Fernie GR, et al. Design of an intervertebral disc prosthesis. Spine 1991;16:S256-60.

8. Hart LG, Deyo RA, Cherkin DC. Physician office visits for low back pain. Frequency, clinical evaluation, and treatment patterns from a U.S. national survey. Spine 1995;20:11-9.

9. Mirza SK, Deyo RA. Systematic review of randomized trials comparing lumbar fusion surgery to nonoperative care for treatment of chronic back pain. Spine 2007;32:816-23.

10. Fritzell P, Hagg O, Jonsson D, et al. Cost-effectiveness of lumbar fusion and nonsurgical treatment for chronic low back pain in the Swedish Lumbar Spine Study: a

multicenter, randomized, controlled trial from the Swedish Lumbar Spine Study Group. Spine 2004;29:421-34; discussion Z3.

11. Blumenthal S, McAfee PC, Guyer RD, et al. A prospective, randomized, multicenter Food and Drug Administration investigational device exemptions study of lumbar total disc replacement with the CHARITE artificial disc versus lumbar fusion: part I: evaluation of clinical outcomes. Spine 2005;30:1565-75; discussion E387-91.

12. Zigler J, Delamarter R, Spivak JM, et al. Results of the prospective, randomized, multicenter Food and Drug Administration investigational device exemption study of the ProDisc-L total disc replacement versus circumferential fusion for the treatment of 1-level degenerative disc disease. Spine 2007;32:1155-62; discussion 63.

13. Hellier WG, Hedman TP, Kostuik JP. Wear studies for development of an intervertebral disc prosthesis. Spine 1992;17:S86-96.

14. Lin EL, Wang JC. Total disk arthroplasty. J Am Acad Orthop Surg 2006;14:705-14.

15. Katta JK, Marcolongo M, Lowman A, et al. Friction and wear behavior of poly(vinyl alcohol)/poly(vinyl pyrrolidone) hydrogels for articular cartilage replacement. J Biomed Mater Res A 2007;83:471-9.

16. Kobayashi M, Toguchida J, Oka M. Development of an artificial meniscus using polyvinyl alcohol-hydrogel for early return to, and continuance of, athletic life in sportspersons with severe meniscus injury. II: animal experiments. Knee 2003;10:53.

17. Kobayashi M, Toguchida J, Oka M. Development of an artificial meniscus using polyvinyl alcohol-hydrogel for early return to, and continuance of, athletic life in sportspersons with severe meniscus injury. I: mechanical evaluation. Knee 2003;10:47-51.

18. Kobayashi M, Toguchida J, Oka M. Preliminary study of polyvinyl alcohol-hydrogel (PVA-H) artificial meniscus. Biomaterials 2003;24:639-47.

19. Oka M, Noguchi T, Kumar P, et al. Development of an artificial articular cartilage. Clin Mater 1990;6:361-81.

20. Noguchi T, Yamamuro T, Oka M, et al. Poly(vinyl alcohol) hydrogel as an artificial articular cartilage: Evaluation of biocompatibility. Journal of Applied Biomaterials 2004;2:101-7.

21. Hassan CM, Ward JH, Peppas NA. Modeling of crystal dissolution of poly(vinyl alcohol) gels produced by freezing/thawing processes. Polymer 2000;41:6729-39.

22. Hyon SH, Cha WI, Ikada Y, et al. Poly(vinyl alcohol) hydrogels as soft contact lens material. J Biomater Sci Polym Ed 1994;5:397-406.

23. Kita M, Ogura Y, Honda Y, et al. Evaluation of polyvinyl alcohol hydrogel as a soft contact lens material. Graefes Arch Clin Exp Ophthalmol 1990;228:533-7.

24. Kita M, Ogura Y, Honda Y, et al. [A polyvinyl alcohol (PVA) hydrogel as a soft contact lens material]. Nippon Ganka Gakkai Zasshi 1990;94:480-3.

25. Di Martino A, Vaccaro AR, Lee JY, et al. Nucleus pulposus replacement: basic science and indications for clinical use. Spine 2005;30:S16-22.

26. Bao QB, Yuan HA. New technologies in spine: nucleus replacement. Spine 2002;27:1245-7.

27. Allen MJ, Schoonmaker JE, Bauer TW, et al. Preclinical evaluation of a poly (vinyl alcohol) hydrogel implant as a replacement for the nucleus pulposus. Spine 2004;29:515-23.

28. Best BA, Guilak F, Setton LA, et al. Compressive mechanical properties of the human anulus fibrosus and their relationship to biochemical composition. Spine 1994;19:212-21.

29. Brown T, Hansen RJ, Yorra AJ. Some mechanical tests on the lumbosacral spine with particular reference to the intervertebral discs; a preliminary report. J Bone Joint Surg Am 1957;39-A:1135-64.

30. Cappozzo A. Compressive loads in the lumbar vertebral column during normal level walking. J Orthop Res 1984;1:292-301.

31. Wan WK, Campbell G, Zhang ZF, et al. Optimizing the tensile properties of polyvinyl alcohol hydrogel for the construction of a bioprosthetic heart valve stent. J Biomed Mater Res 2002;63:854-61.

32. Burns ML, Kaleps I, Kazarian LE. Analysis of compressive creep behavior of the vertebral unit subjected to a uniform axial loading using exact parametric solution equations of Kelvin-solid models--Part I. Human intervertebral joints. J Biomech 1984;17:113-30.

33. Kaleps I, Kazarian LE, Burns ML. Analysis of compressive creep behavior of the vertebral unit subjected to a uniform axial loading using exact parametric solution equations of Kelvin-solid models--Part II. Rhesus monkey intervertebral joints. J Biomech 1984;17:131-6.

34. Keller TS, Spengler DM, Hansson TH. Mechanical behavior of the human lumbar spine. I. Creep analysis during static compressive loading. J Orthop Res 1987;5:467-78.

35. Meyers MA, Chawla KK. Mechanial Behavior of Materials. 1999:98-103.

36. McCrum NG, Buckley CP, Bucknell CB. Principles of Polymer Engineering. 2003:117-76.

37. Mow VC, Proctor CS, Kelly MA, et al. Chapter 2 - Biomechanics of articular cartilage. Basic Biomechanics of the Musculoskeletal System, Second Edition 1989:31-54.

38. Hassan CM, Peppas NA. Structure and morphology of freeze/thawed PVA hydrogels. Macromolecules 2000;33:2472-9.

39. Lozinsky VI, Damshkaln LG, Shaskol'skii BL, et al. Study of cryostructuring of polymer systems: 27. Physicochemical properties of poly(vinyl alcohol) cryogels and specific features of their macroporous morphology. Colloid Journal 2007;69:747-64.

40. Auriemma F, De Rosa C, Ricciardi R, et al. Time-resolving analysis of cryotropic gelation of water/poly(vinyl alcohol) solutions via small-angle neutron scattering. J Phys Chem B 2008;112:816-23.

41. Sakalkale DP, Bhagia SA, Slipman CW. A historical review and current perspective on the intervertebral disc prosthesis. Pain Physician 2003;6:195-8.

42. Spiliopoulou I, Korovessis P, Konstantinou D, et al. IgG and IgM concentration in the prolapsed human intervertebral disc and sciatica etiology. Spine 1994;19:1320-3.

43. Buckwalter JA. Aging and degeneration of the human intervertebral disc. Spine 1995;20:1307-14.

44. Klara PM, Ray CD. Artificial nucleus replacement: clinical experience. Spine 2002;27:1374-7.

45. McGlashen KM, Miller JA, Schultz AB, et al. Load displacement behavior of the human lumbo-sacral joint. J Orthop Res 1987;5:488-96.

46. Virgin WJ. Experimental investigations into the physical properties of the intervertebral disc. J Bone Joint Surg Br 1951;33-B:607-11.

47. Ebara S, Iatridis JC, Setton LA, et al. Tensile properties of nondegenerate human lumbar anulus fibrosus. Spine 1996;21:452-61.

48. Yaszenmski MJ, White AA, Panjabi MM. Chapter 3: Biomechanics of the Spine. Orthopaedic Knowledge Update – Spine 2nd Edition 1996:15-23.

49. Koeller W, Muehlhaus S, Meier W, et al. Biomechanical properties of human intervertebral discs subjected to axial dynamic compression--influence of age and degeneration. J Biomech 1986;19:807-16.

50. Skaggs DL, Weidenbaum M, Iatridis JC, et al. Regional variation in tensile properties and biochemical composition of the human lumbar anulus fibrosus. Spine 1994;19:1310-9.

51. Galante JO. Tensile properties of the human lumbar annulus fibrosus. Acta Orthop Scand 1967:Suppl 100:1-91.

52. Cloyd JM, Malhotra NR, Weng L, et al. Material properties in unconfined compression of human nucleus pulposus, injectable hyaluronic acid-based hydrogels and tissue engineering scaffolds. Eur Spine J 2007.

53. Elliott DM, Sarver JJ. Young investigator award winner: validation of the mouse and rat disc as mechanical models of the human lumbar disc. Spine 2004;29:713-22.

54. Iatridis JC, Setton LA, Weidenbaum M, et al. Alterations in the mechanical behavior of the human lumbar nucleus pulposus with degeneration and aging. J Orthop Res 1997;15:318-22.

55. Iatridis JC, Weidenbaum M, Setton LA, et al. Is the nucleus pulposus a solid or a fluid? Mechanical behaviors of the nucleus pulposus of the human intervertebral disc. Spine 1996;21:1174-84.

56. Bushell GR, Ghosh P, Taylor TF, et al. Proteoglycan chemistry of the intervertebral disks. Clin Orthop Relat Res 1977:115-23.

57. Setton LA, Zhu W, Weidenbaum M, et al. Compressive properties of the cartilaginous end-plate of the baboon lumbar spine. J Orthop Res 1993;11:228-39.

58. Oka M. Biomechanics and repair of articular cartilage. J Orthop Sci 2001;6:448-56.

59. Nachemson A. Lumbar intradiscal pressure. Experimental studies on post-mortem material. Acta Orthop Scand Suppl 1960;43:1-104.

60. Hirsch C, Schajowica F. Studies on structural changes in the lumbar annulus fibrosus. Acta orthop. Scand 1952:184.

Table 1. Summary of Tangent Compressive Elastic Modulus Values for PVA-C*

	PVA Concentration					
Parameters	**3%PVA**	**5%PVA**	**15%PVA**	**25%PVA**	**35%PVA**	**40%PVA**
1 FTC						
EM at 5% Strain (MPa)	0.001	0.003	0.089	0.197	0.501	0.950
EM at 20% Strain (MPa)	0.001	0.006	0.138	0.465	0.941	1.521
3 FTC						
EM at 5% Strain (MPa)	0.002	0.020	0.253	0.517	0.781	0.950
EM at 20% Strain (MPa)	0.001	0.043	0.425	0.822	1.413	2.061
6 FTC						
EM at 5% Strain (MPa)	0.007	0.046	0.357	0.523	0.904	1.303
EM at 20% Strain (MPa)	0.013	0.080	0.669	0.863	1.753	2.117

*EM = Elastic modulus

Table 2. Summary of Stress Relaxation Results for All PVA-C Formulations*

	PVA Concentration					
Parameters	**3%PVA**	**5%PVA**	**15%PVA**	**25%PVA**	**35%PVA**	**40%PVA**
1 FTC						
Inst. relax rate (Pa/s)	30	40	600	7300	23700	69300
S.S. relax rate (Pa/s)	0.2	0.2	7	10	50	90
% Change Stress	19.2±4.9	5.0±7.4	3.7±2.3	6.9±0.4	7.8±0.8	17.1±1.5
k_1 (sec^{-1})	1.79±0.45	1.52±0.50	1.65±0.07	2.13±0.14	4.04±0.06	1.99±0.04
k_2 (sec^{-1})	0.100±0.006	0.106±0.007	0.114±0.001	0.074±0.005	0.097±0.001	0.114±0.002
3 FTC						
Inst. relax rate (Pa/s)	30	300	1500	31400	78900	83300
S.S. relax rate (Pa/s)	0.4	5	30	50	100	100
% Change Stress	9.7±3.0	6.9±3.3	3.8±0.6	12.4±0.9	5.6±2.3	13.5±0.5
k_1 (sec^{-1})	1.88±0.44	1.10±0.04	1.60±0.09	2.11±0.05	2.25±0.04	2.37±0.05
k_2 (sec^{-1})	0.080±0.004	0.082±0.001	0.090±0.001	0.129±0.002	0.123±0.002	0.106±0.001
6 FTC						
Inst. relax rate (Pa/s)	100	500	4600	39400	94200	109500
S.S. relax rate (Pa/s)	2	9	70	40	100	100
% Change Stress	8.9±6.2	6.3±2.0	5.2±1.7	10.9±0.3	15.7±2.6	16.9±0.6
k_1 (sec^{-1})	2.31±0.49	1.57±0.09	2.31±0.13	1.98±0.06	3.11±0.07	2.32±0.04
k_2 (sec^{-1})	0.106±0.003	0.106±0.001	0.097±0.001	0.112±0.002	0.130±0.002	0.130±0.002

*Inst.=Instantaneous, S.S.=Steady state, sec=seconds. The instantaneous stress relaxation rates were calculated immediately after loading, and the final stress relaxation rates were calculated at 30 seconds. The percent changes in stress were calculated with stress at t=0 in the denominator.

Table 3. Summary of Creep Results for All PVA-C Formulations*

	PVA Concentration					
Parameters	**3%PVA**	**5%PVA**	**15%PVA**	**25%PVA**	**35%PVA**	**40%PVA**
1 FTC						
Inst. creep rate (sec^{-1})			0.0015	0.003	0.0052	0.003
S.S. creep rate (sec^{-1})			1.0E-05	2.0E-05	4.0E-05	4.0E-05
% Change Strain			1.4±0.9	2.1±0.7	2.9±1.7	3.1±1.6
E_1 (MPa)			7.82±0.18	21.36±0.38	38.10±0.71	41.91±0.62
E_2 (MPa)			0.107±0	0.351±0.0001	0.691±0.0002	0.921±0.0003
η (MPa)			132.1±5.1	52.0±2.2	218.9±11.0	315.1±14.0
3 FTC						
Inst. creep rate (sec^{-1})		0.016	0.0066	0.0055	0.0054	0.0018
S.S. creep rate (sec^{-1})		7.0E-05	4.0E-05	2.0E-05	6.0E-05	4.0E-05
% Change Strain		8.8±4.0	3.6±1.5	2.0±0.7	3.6±2.7	2.4±3.9
E_1 (MPa)		0.71±0.02	11.92±0.09	31.86±0.53	40.25±0.64	63.22±0.87
E_2 (MPa)		0.035±0.0004	0.330±0.0001	0.612±0.0002	0.950±0.0003	1.096±0.001
η (MPa)		5.2±0.3	44.5±0.9	96.1±3.8	240.9±10.5	383.5±14.6
6 FTC						
Inst. creep rate (sec^{-1})	0.013	0.0078	0.0016	0.0049	0.0019	0.0044
S.S. creep rate (sec^{-1})	8.0E-05	8.0E-06	5.0E-05	3.0E-05	4.0E-05	2.0E-05
% Change Strain	17.0±1.2	1.5±4.4	2.5±3.0	2.0±1.5	2.2±2.4	1.8±0.2
E_1 (MPa)	0.080±0.001	8.55±0.48	24.93±0.38	37.87±0.65	62.80±0.84	59.83±0.75
E_2 (MPa)	0.012±0	0.063±0	0.516±0.0001	0.657±0.0002	1.056±0	1.112±0
η (MPa)	0.3±0	13.2±1.7	102.3±4.0	126.4±5.2	451.9±17.6	488.9±12.0

*Inst.=Instantaneous, S.S.=Steady state, sec=seconds, $E=10^x$. The compressive creep test was carried out to a force corresponding to 3mm or 223N which ever is lower. The instantaneous creep rates were calculated immediately after loading, and the final creep rates were calculated at 30 seconds. The percent changes in strain were calculated with stain at t=0 in the denominator.

Table 4. Comparison of Material Property between PVA-C and Human Lumbar IVD*

	Human IVD	PVA-C		Suitable Formuation(s)	
	Range	Min.	Max.	Formulation	Value
Compression					
Annulus Fibrosus [4,28,29,45-47,50,51,53,59,60]					
Initial EM at ~5% strain (MPa)	2.9-6.6	0.0007	1.303	None	
Linear EM at ~20% strain (MPa)	21.2-27.5	0.001	2.117	None	
Nucleus Pulposus [29,52,55]					
Initial EM at ~5% strain (MPa)	0.00169-0.00481	0.0007	1.303	**3% 3FTC**	**0.002**
				5% 1FTC	**0.0026**
Linear EM at ~20% strain (MPa)	0.00283-0.00795	0.001	2.117	**3% 3FTC**	**0.0031**
				5% 1FTC	**0.0055**
Stress Relaxation (whole disc) [4]					
SS Relaxation Rate† (Pa/s)	0-120	0.2	100	All	
% Decrease in Stress†	46%-67%	3.7±2.3%	19.2±4.9%	All	
Creep‡ (whole disc) [4,34]					
SS Creep Rate† (sec^{-1})	$5x10^{-6}$-$1.3\ x10^{-5}$	$8x10^{-6}$	$8x10^{-5}$	All	
% Increase in Strain†	30%-108%	1.4±0.9%	17.0±0.2%	All	
E_1 (MPa)	4.204-10.48	0.080±0.001	63.22±0.87	*5% 6FTC*	*8.55±0.48*
				15% 1FTC	*7.82±0.18*
E_2 (MPa)	1.057-2.245	0.0119±0.00003	1.112±0.001	*40% 3FTC*	*1.096±0.001*
				40% 6FTC	*1.112±0.001*
η (MPa/s)	2590-16090	0.313±0.013	488.9±25	*None*	

*EM = Elastic Modulus, SS = Steady State, †=Human values at >30min, ‡ = Limited PVA-C set. Non-standardized units for load and displacement (e.g. pounds and inches) were converted to stress and strain based on the best estimate of normal human IVD dimensions. Compressive elastic modulus values were available for the annulus fibrosus and the nucleus pulposus. Stress relaxation and creep could only be found for the entire disc.

Figure Legend

Figure 1. Typical stress-strain hysteresis curves at 3mm displacement loading (15%PVA-C with 1, 3 and 6 freeze-thaw cycles).

Figure 2. Histogram of initial compressive tangent elastic modulus at 5% strain for all PVA-C formulations. The elastic modulus increased with either increasing PVA concentration or number of FTC's.

Figure 3. Histogram of large compressive tangent elastic modulus at 20% strain for all PVA-C formulations. The elastic modulus increased with either increasing PVA concentration or number of FTC's.

Figure 4. Typical stress relaxation data (35%-3FTC sample) accompanied by its fitted curve from Equation 1 using 3mm initial displacement.

Figure 5. Histogram of instantaneous stress relaxation rates for all PVA-C formulations with 3mm initial displacement.

Figure 6. Typical creep data (15%-3FTC sample) accompanied by its fitted curve from Equation 2 using a force-equivalence of 3mm displacement.

Figure 7. Histogram of E_1 values (viscous modulus) for all PVA-C formulations (except for samples noted in text). See Equation 2 for details.

Figure 8. Histogram of E_2 values (instantaneous modulus) for all PVA-C formulations (except for samples noted in text). See Equation 2 for details.

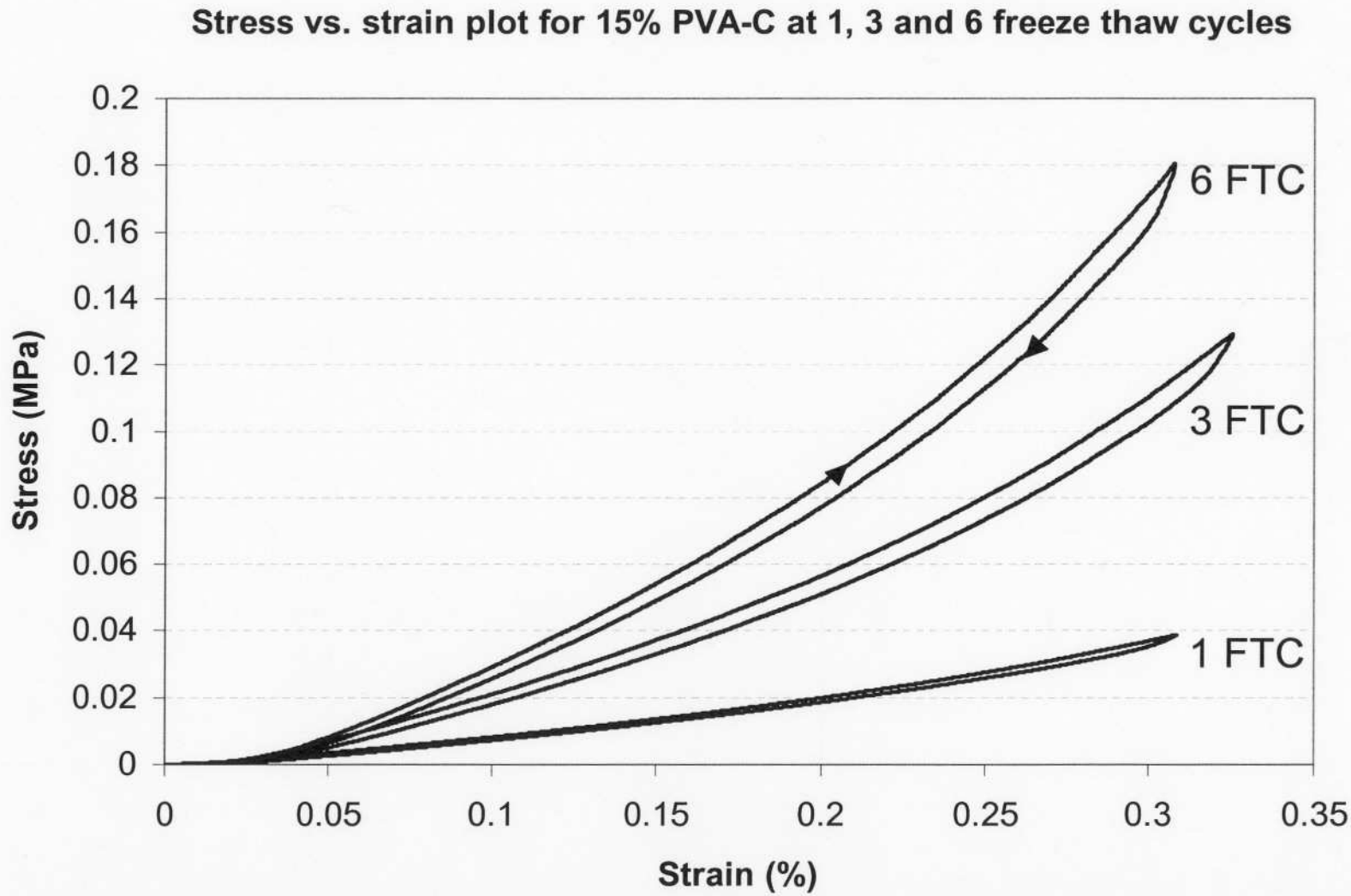
Stress vs. strain plot for 15% PVA-C at 1, 3 and 6 freeze thaw cycles
Stress (MPa)
0.2
0.18
0.16
0.14
0.12
0.1
0.08
0.06
0.04
0.02
0
0
0.05
0.1
0.15
0.2
0.25
0.3
0.35
Strain (%)
6 FTC
3 FTC
1 FTC

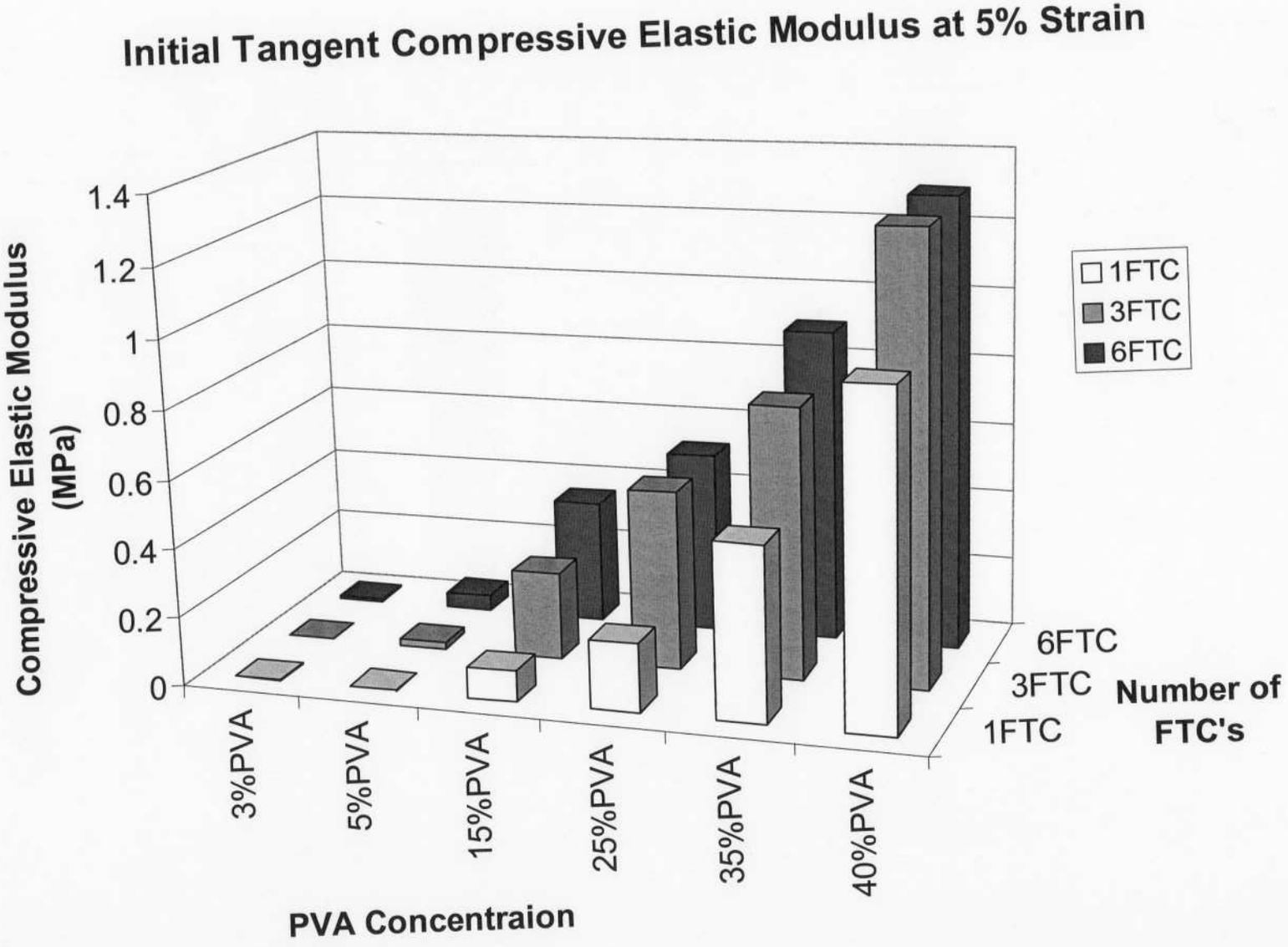
Initial Tangent Compressive Elastic Modulus at 5% Strain
Compressive Elastic Modulus (MPa)
1.4
1.2
1
0.8
0.6
0.4
0.2
0
1FTC
3FTC
6FTC
6FTC
3FTC
1FTC
Number of FTC's
3%PVA
5%PVA
15%PVA
25%PVA
35%PVA
40%PVA
PVA Concentraion

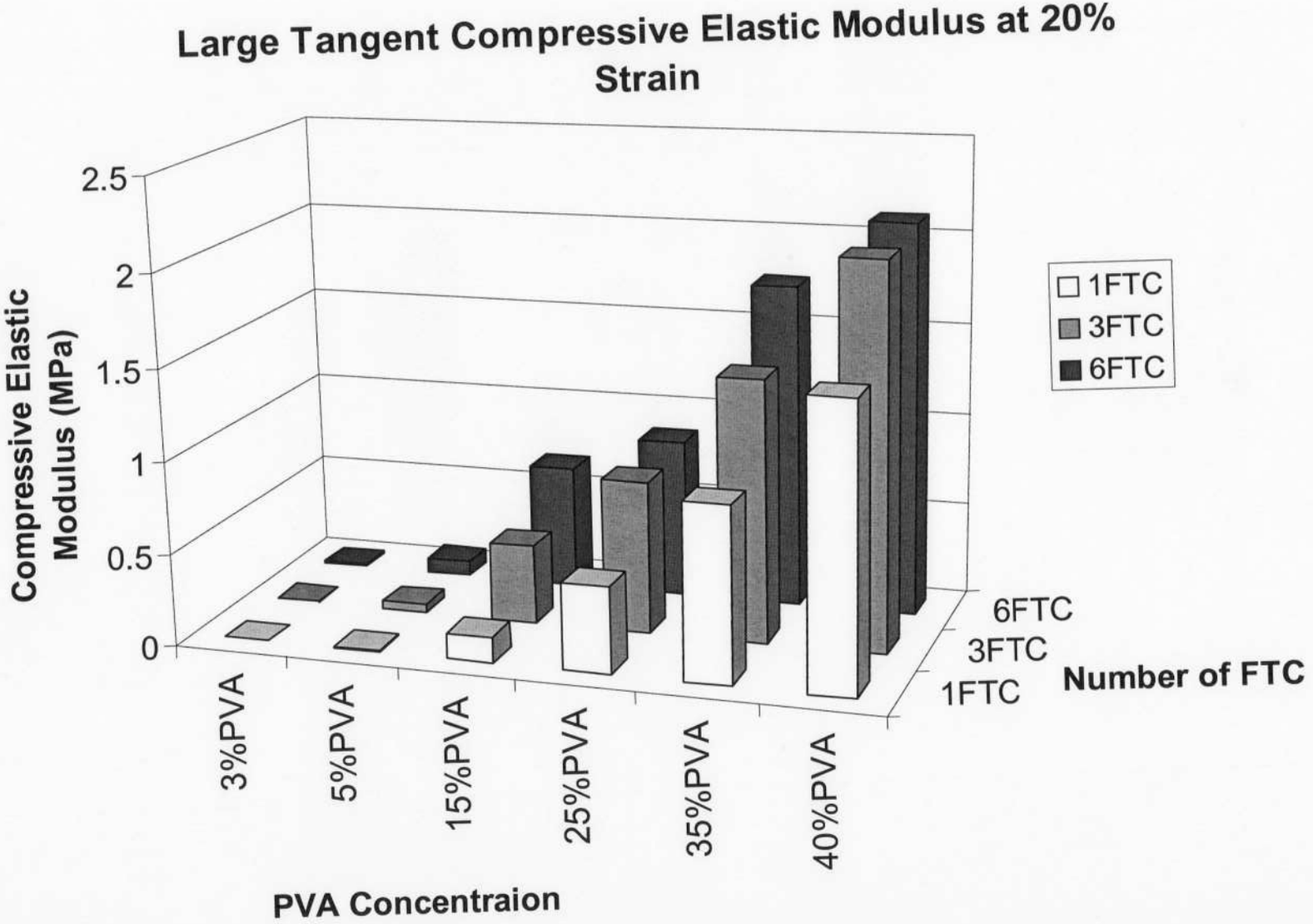
Large Tangent Compressive Elastic Modulus at 20% Strain
Compressive Elastic Modulus (MPa)
2.5
2
1.5
1
0.5
0
1FTC
3FTC
6FTC
6FTC
3FTC
1FTC
Number of FTC
3%PVA
5%PVA
15%PVA
25%PVA
35%PVA
40%PVA
PVA Concentraion

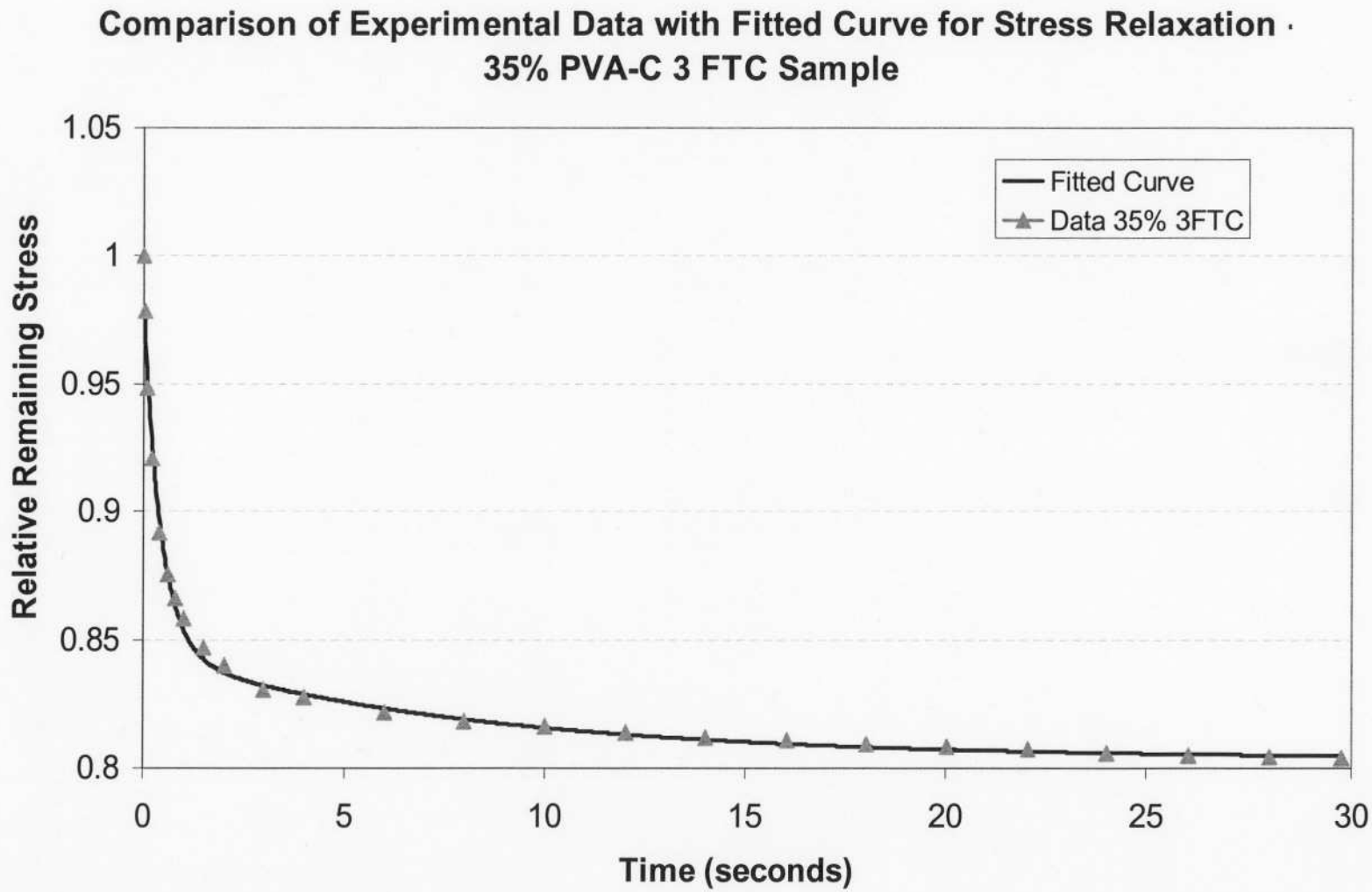
Comparison of Experimental Data with Fitted Curve for Stress Relaxation · 35% PVA-C 3 FTC Sample
Relative Remaining Stress
1.05
1
0.95
0.9
0.85
0.8
0
5
10
15
20
25
30
Time (seconds)
Fitted Curve
Data 35% 3FTC

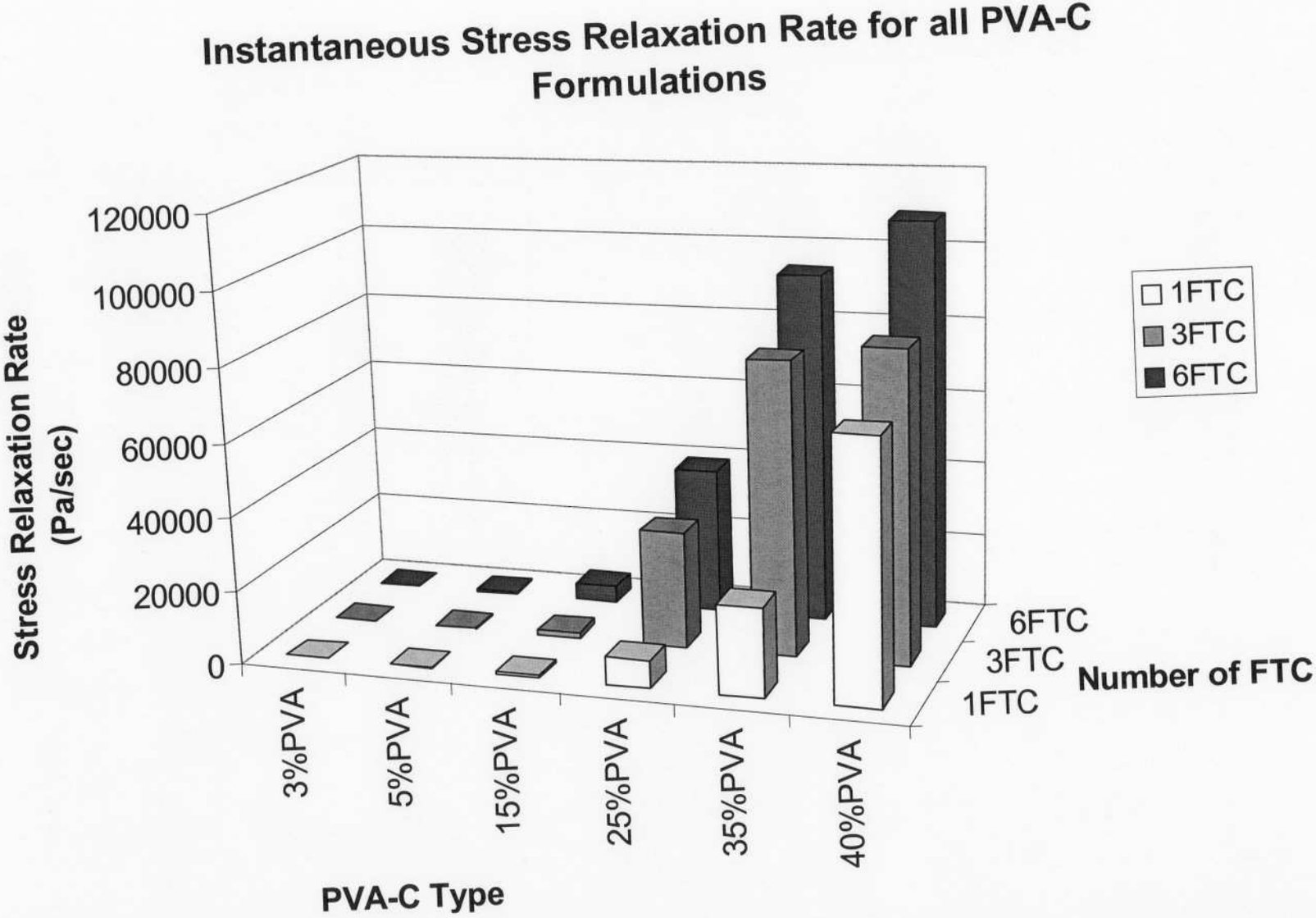
Instantaneous Stress Relaxation Rate for all PVA-C Formulations
Stress Relaxation Rate (Pa/sec)
120000
100000
80000
60000
40000
20000
0
3%PVA
5%PVA
15%PVA
25%PVA
35%PVA
40%PVA
PVA-C Type
1FTC
3FTC
6FTC
Number of FTC

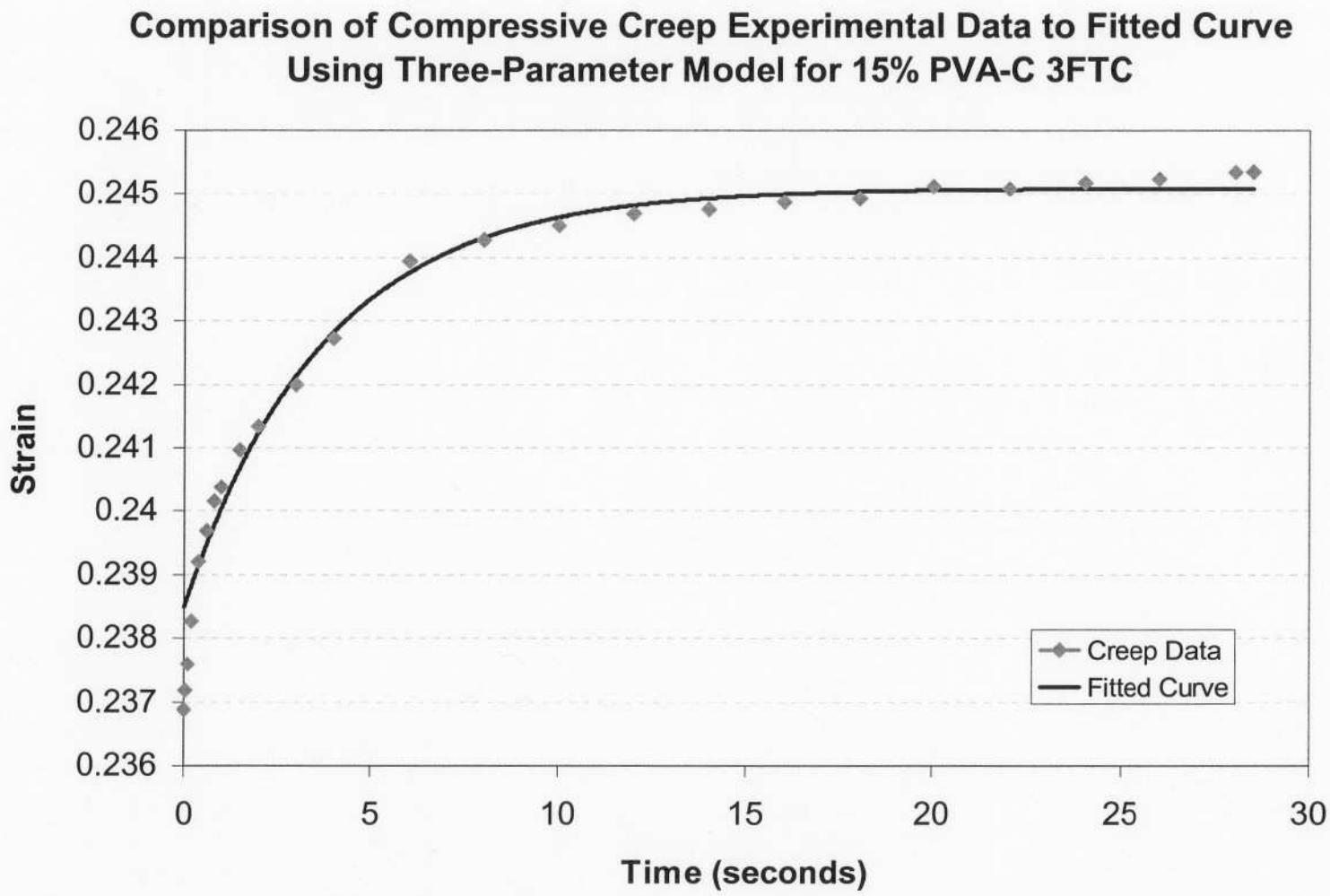
Comparison of Compressive Creep Experimental Data to Fitted Curve
Using Three-Parameter Model for 15% PVA-C 3FTC
Strain
0.246
0.245
0.244
0.243
0.242
0.241
0.24
0.239
0.238
0.237
0.236
0
5
10
15
20
25
30
Time (seconds)
Creep Data
Fitted Curve

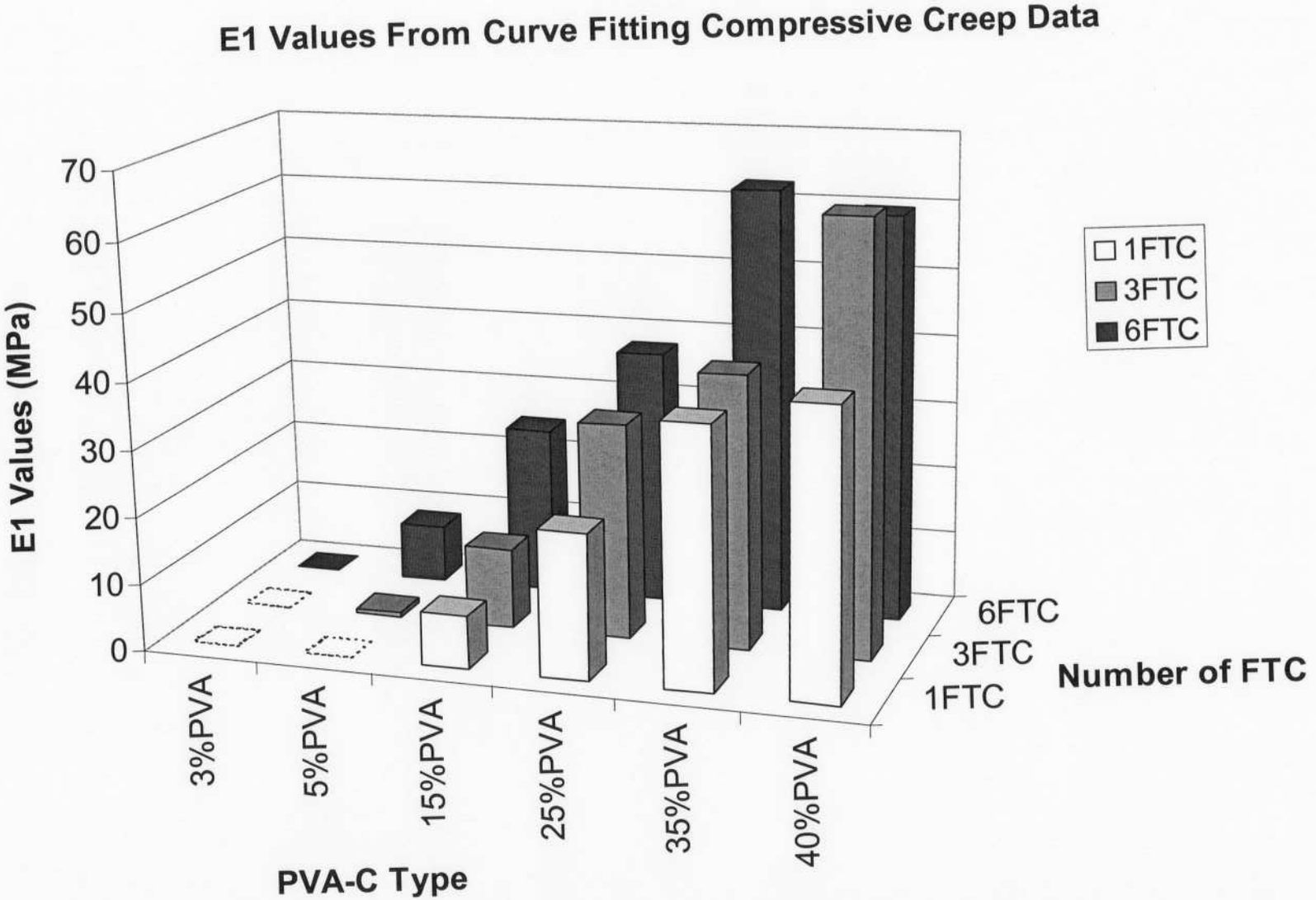
E1 Values From Curve Fitting Compressive Creep Data
E1 Values (MPa)
70
60
50
40
30
20
10
0
1FTC
3FTC
6FTC
6FTC
3FTC
1FTC
Number of FTC
3%PVA
5%PVA
15%PVA
25%PVA
35%PVA
40%PVA
PVA-C Type

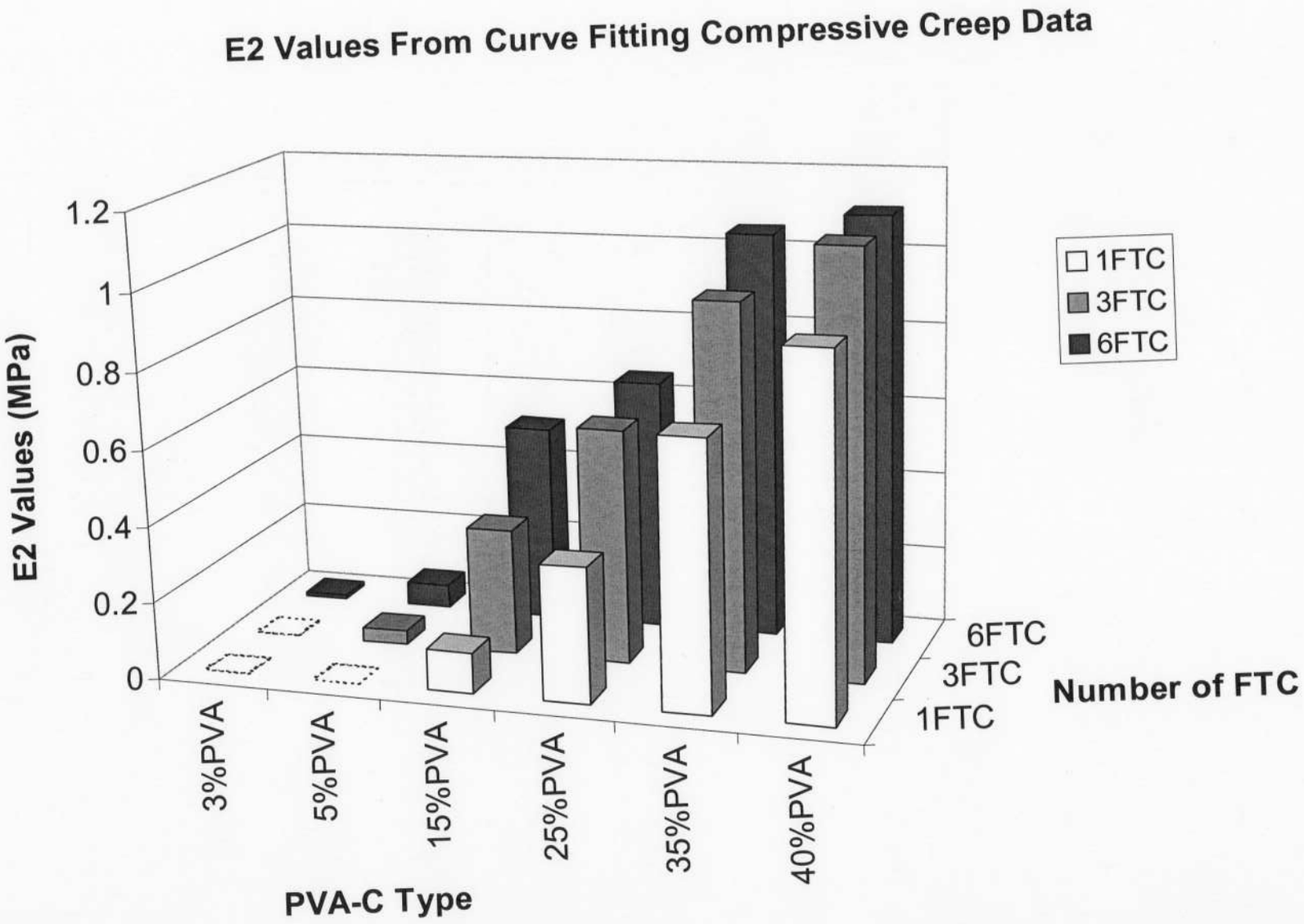
E2 Values From Curve Fitting Compressive Creep Data
E2 Values (MPa)
1.2
1
0.8
0.6
0.4
0.2
0
1FTC
3FTC
6FTC
6FTC
3FTC
1FTC
Number of FTC
3%PVA
5%PVA
15%PVA
25%PVA
35%PVA
40%PVA
PVA-C Type